ACADEMIC PRESS

Available online at www.sciencedirect.com

SCIENCE DIRECT®

Journal of Magnetic Resonance 164 (2003) 228–232

JMR Journal of Magnetic Resonance

www.elsevier.com/locate/jmr

LR-CAHSQC: an application of a Carr–Purcell–Meiboom–Gill-type sequence to heteronuclear multiple bond correlation spectroscopy

Harri Koskela,[a,*] Ilkka Kilpeläinen,[a] and Sami Heikkinen[b]

[a] *Department of Chemistry, University of Oulu, P.O. Box 3000, Oulu FIN-90014, Finland*
[b] *Department of Radiology, Helsinki University Central Hospital, P.O. Box 340, HUS FIN-00029, Finland*

Received 6 March 2003; revised 26 June 2003

Abstract

A new pulse sequence, long-range CPMG-adjusted heteronuclear single quantum coherence (LR-CAHSQC), is proposed for the determination of long-range J_{CH} coupling constants from a long-range ^{1}H–^{13}C correlation experiment. The long-range heteronuclear coupling constants can be directly extracted from COSY-type antiphase peak patterns. The current approach utilizes CPMG-sequences for polarization transfer, and thus avoids the evolution of homonuclear J_{HH} couplings, which normally may introduce abnormalities into the cross peak pattern. The differences between LR-CAHSQC and normal LR-HSQC are discussed.

Keywords: 2D NMR; Heteronuclear long-range coupling constants; CPMG; HSQC

1. Introduction

Long-range heteronuclear ^{1}H–^{13}C coupling constants provide valuable information about molecular structure and conformation. Therefore, a multitude of techniques to extract long-range heteronuclear coupling constants from different types of NMR spectra have been developed. A common approach is to utilize long-range ^{1}H–^{13}C correlation experiments, which allow the detection of spectra with a good sensitivity combined with good resolution. Here, a traditional tool is HMBC [1], which can provide qualitative information about the long-range heteronuclear couplings. However, accurate coupling constant measurements with HMBC sequences are relatively difficult, as homonuclear J_{HH} evolution causes twisted correlation peak shapes [2–5].

An alternative approach is to utilize long-range versions of HSQC [6–8]. In principle, with HSQC-based techniques, the correlation peak shapes can be improved, as no J_{HH} evolution takes place during t_1. Improved phase properties allow the use of normal 1D spectra as a reference in favorable cases. However, the J_{HH} evolution is active during the long polarization transfer delays of the INEPT, and some of the magnetization will be transferred to homonuclear multiple-quantum coherence [9]. This coherence can become observable later in the pulse sequence and contribute to the multiplet shape making the coupling constant evaluation more difficult (vide infra).

The CPMG-pulse train [10,11] is commonly applied in T_2-relaxation measurements [12–15]. In addition, under certain experimental conditions, the *J*-evolution during the CPMG pulse train can be avoided [16,17]. When CPMG-sequence is conducted simultaneously on two heterospins (CPMG–INEPT), the heteronuclear couplings will evolve, but homonuclear coupling (J_{HH}) evolution is suppressed. We have adapted CPMG-sequence to replace the INEPT periods of LR-HSQC. In the current CPMG-based approach, the J_{HH} evolution is effectively suppressed during polarization transfer periods, and long-range ^{1}H–^{13}C correlation spectra can be acquired with good intensity and clean phase properties.

The original CPMG-train with a single phase for the 180° pulses focuses the magnetization along the same axis along which the pulses are applied, but quickly

* Corresponding author. Fax: +358-8-553-1603.
E-mail address: Harri.Koskela@oulu.fi (H. Koskela).

1090-7807/$ - see front matter © 2003 Elsevier Inc. All rights reserved.
doi:10.1016/S1090-7807(03)00250-7

dephases the magnetization on the other cartesian coordinate axes due to the spatial inhomogeneity of B_1-field. As the polarization is transferred from the proton in-phase term H_y to the antiphase term H_xC_z, the applied CPMG-sequence should be equally effective regardless of the magnetization orientation on the cartesian coordinates. Therefore, the XY-16 sequence [18], which preserves the magnetization on all axes, was selected for its usefulness on polarization transfer and suppression of J_{HH} couplings. The influence of homonuclear Hartmann–Hahn transfer [19] is also discussed.

It should be noted that CPMG–INEPT transfer should not be mixed with HEHAHA [20–22], as the Hartmann–Hahn condition $\gamma_H B_{1H} = \gamma_C B_{1C}$ needs not to be fulfilled, and the polarization transfer from proton to carbon is purely due to the J_{CH} evolution. The concept presented here has been previously applied to the HSQC-experiments involving ^{31}P as a X-nuclei [23], and to biomolecules to improve the detection of fast-exchanging protons [24,25], but to the best of our knowledge has not been used for heteronuclear multiple-bond correlation spectroscopy.

2. Description of the method

The pulse sequence for LR-CAHSQC is presented in Fig. 1a. The pulse sequence for LR-CAHSQC is essentially similar to LR-HSQC (Fig. 1b), but the INEPT polarization transfer has been replaced with a CPMG-sequence. The suppression of one-bond correlations is carried out using a double-tuned low-pass PFG-z-filter [26]. Polarization is transferred from proton to carbon using CPMG–INEPT period matched for heteronuclear long-range couplings. The CPMG–INEPT period consists of a number of XY-16 sequences with total duration of $1/(2\,{}^nJ_{CH})$. In order to avoid the evolution of the J_{HH} couplings during the CPMG–INEPT periods, it is essential to select the τ delay short enough.

According to a homonuclear two-spin study by Wells and Gutowsky [27], it is possible to suppress the evolution of the J_{HH} couplings during CPMG-pulse train by fast 180° pulse repetition. For a successful suppression of the J_{HH} evolution, the delay τ should be smaller than $1/(2\sqrt{J^2 + \Delta\nu^2})$. For weakly coupled spin systems, the approximated condition $\tau < 1/(2\Delta\nu_{max})$, where $\Delta\nu_{max}$ is largest shift difference of the coupled spins encountered, is sufficient. The lower limit of τ is defined by the duty cycle at which the spectrometer can operate safely. It should be noted that from the point of suppression of J-evolution, a low B_0 field strength can be considered beneficial, because the reduced $\Delta\nu_{max}$ value enables efficient suppression of J-evolution without need for very short τ-values, thus leading to a lower duty cycle.

Although the J_{HH} coupling evolution is suppressed during the CPMG-sequence, polarization is transferred between protons by homonuclear Hartmann–Hahn transfer [28–30]. According to the study of Braunschweiler and Ernst [28], a closely spaced 180° pulse train is quite effective at such transfer, and polarization will be transferred between protons of HH′ spin system through J-coupling by isotropic mixing:

$$\begin{aligned} H_x \overset{\overline{H}J\tau_m}{\rightarrow} & 1/2H_x\{1+\cos(2\pi J_{HH'}\tau_m)\} \\ & + 1/2H'_x\{1-\cos(2\pi J_{HH'}\tau_m)\} \\ & + \left(H_yH'_z - H_zH'_y\right)\sin(2\pi J_{HH'}\tau_m), \end{aligned} \quad (1)$$

where $\overline{H}$ is the isotropic mixing Hamiltonian and τ_m is the mixing time. Thus, Hartmann–Hahn transfer between protons can be expected during the CPMG–INEPT period. Because the shift difference between carbons and protons is very large, the J-suppression does not apply to couplings between proton and carbon. Consequently, heteronuclear coupling is active, and the

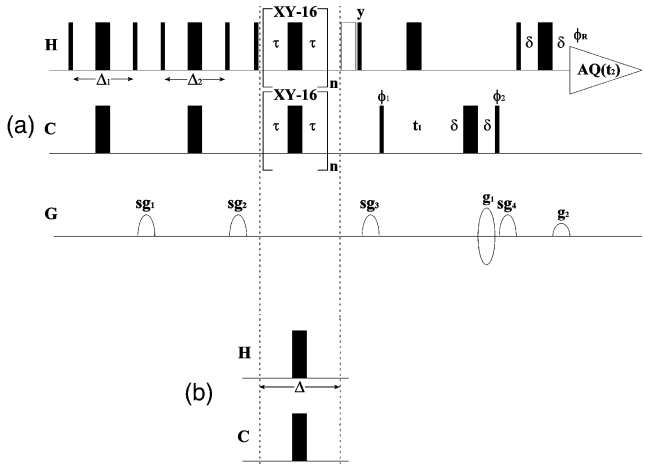

Fig. 1. Pulse sequence for LR-CAHSQC in which INEPT is replaced by a CPMG-train (a) and LR-HSQC with normal INEPT (b). Narrow and thick bars represents the 90° and 180° RF-pulses, respectively. The 90° pulse durations are 6.0 μs for ^1H and 11.6 μs for ^{13}C. The unfilled rectangle represents a spin-lock pulse (1.5 ms). The pulse phases are along x if not indicated otherwise. Phase cycles are: $\phi_1 = \{x, -x\}$, $\phi_2 = \{x, x, -x, -x\}$, and $\phi_R = \{x, -x, -x, x\}$. The pulse phases in the XY-16 sequence are: $\{x, y, x, y, y, x, y, x, -x, -y, -x, -y, -y, -x, -y, -x\}$. The delays Δ_1 and Δ_2 in the double-tuned low-pass filter are tuned for 169 and 145 Hz, respectively. The long-range polarization transfer delay Δ in LR-HSQC is optimized to correspond the average ${}^nJ_{CH}$ coupling constant in sucrose. The τ is set to approximately 200 μs for LR-CAHSQC. The number of cycles (n) in LR-CAHSQC is set so that the duration of consecutive XY-16 cycles equals with long-range polarization transfer delay Δ, and τ is further fine-tuned in order to fulfill this condition. The pulsed field gradients are represented by half-ellipses. The PFG duration is 1 ms, with a recovery delay of 100 μs, thus giving 1.1 ms for the delay δ. The applied PFG strengths are: $g1 = 48$ G/cm, $g2 = 12$ G/cm, $sg1 = 36.6$ G/cm, $sg2 = 42.2$ G/cm, $sg3 = 30$ G/cm, and $sg4 = 25$ G/cm (sg = spoiler gradient). Quadrature detection in the F1-dimension is accomplished with a gradient-based echo–antiecho method by inverting the sign of g_1. The axial peak displacement is achieved with the States–TPPI method by inverting the phases ϕ_1 and ϕ_R on every second increment of t_1.

antiphase proton magnetization is formed through heteronuclear long-range coupling. When considering the HH′C spin system ($J_{HH'}$, $J_{CH} \neq 0$ and $J_{CH'} = 0$), and taking the homonuclear Hartmann–Hahn transfer during delay Δ into account, the magnetization after the LR-CAHSQC is described by

$$1/2H_yC_z\{1 + \cos(2\pi J_{HH'}\Delta)\} \times \sin(\pi J_{CH}\Delta)\cos(\Omega_C t_1). \quad (2)$$

For comparison, Eq. (3) presents the observable magnetization for HH′C spin system ($J_{HH'}$, $J_{CH} \neq 0$, and $J_{CH'} = 0$) after LR-HSQC pulse sequence

$$-H_yC_z \sin(\pi J_{CH}\Delta)\cos(\pi J_{HH'}\Delta)\cos(\Omega_C t_1). \quad (3)$$

When comparing Eqs. (2) and (3), it is evident that the sign of the observable term in LR-HSQC is dependent on the $J_{HH'}/J_{opt}$ ratio, where the J_{opt} corresponds to the average $^nJ_{CH}$ coupling constant used for the definition of polarization transfer delay. The sign of the term will change when the ratio crosses unity. For the LR-CAHSQC the sign of the term remains the same regardless of ratio $J_{HH'}/J_{opt}$ (Fig. 2). The sign of the term correlates to the phase of the correlation peak, and thus with LR-HSQC the phase will be shifted by 180°, if the $J_{HH'}/J_{opt}$ ratio is larger than 1.

Furthermore, in the case of LR-HSQC, additional protons coupled to the observed proton with $J_{HH'}$s approximately similar to J_{opt} may result in development of more complex magnetization during the INEPT-period, which can render observable in a later stage of the pulse sequence and contribute to the correlation peak shape. The observable magnetization after LR-HSQC arising from the HH′H″C spin system ($J_{HH'}$, $J_{HH''}$, $J_{CH} \neq 0$ and $J_{CH'}$, $J_{CH''} = 0$) is presented as

$$-H_yC_z \sin(\pi J_{CH}\Delta)\cos(\pi J_{HH'}\Delta)\cos(\pi J_{HH''}\Delta) \times \cos(\Omega_C t_1) + H_yH'_zH''_zC_z \sin(\pi J_{CH}\Delta)\sin(\pi J_{HH'}\Delta) \times \sin(\pi J_{HH''}\Delta)\sin(\pi J_{HH'}t_1)\sin(\pi J_{HH''}t_1)\cos(\Omega_C t_1). \quad (4)$$

When $J_{HH'} \approx J_{HH''} \approx J_{opt}$, the term $H_yH'_zH''_zC_z$ can significantly contribute to the multiplet pattern in the spectrum, while the desired magnetization described by the term H_yC_z will approach zero. In summary, these effects in LR-HSQC may severely interfere the spectral quality, and result a spectrum with distorted lineshapes.

3. Results and discussion

The correlation peak shape characteristic and coupling constant evaluation using LR-HSQC and LR-CAHSQC methods were examined by comparing the spectra of sucrose (Fig. 3). The spectra were measured with long-range polarization transfer delay optimized for 5, 10, and 15 Hz ($=J_{opt}$). With these values no phase alteration of the correlation peak due to the heteronuclear long-range coupling evolution is possible, but the effect of homonuclear couplings on the phase of the peak can be monitored. The spectra were phased according to the C^{III},H^I peak ($^3J_{CH}$), as the H^I proton does not have any homonuclear coupling partners. The 1D reference spectra were constructed by subtracting two ^1H spectra with frequency offsets of $+J_{CH}/2$ and

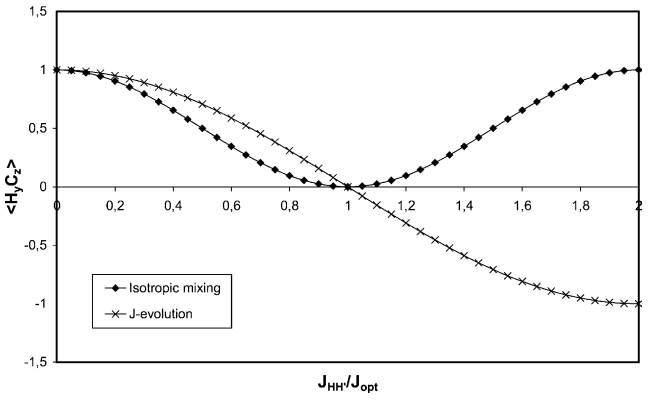

Fig. 2. Plot showing the size of the H_yC_z term (HH′C spin system) for LR-CAHSQC (Eq. (2)) and LR-HSQC (Eq. (3)) as a function of the $J_{HH'}/J_{opt}$ ratio. $J_{HH'}$ is the homonuclear coupling constant, and J_{opt} is the heteronuclear coupling constant for which the polarization transfer delay is optimized. In both cases the intensity is zero when $J_{HH'}/J_{opt} = 1$. For the LR-HSQC the sign of the H_yC_z term is dependent on the ratio, but for the LR-CAHSQC the sign is always positive.

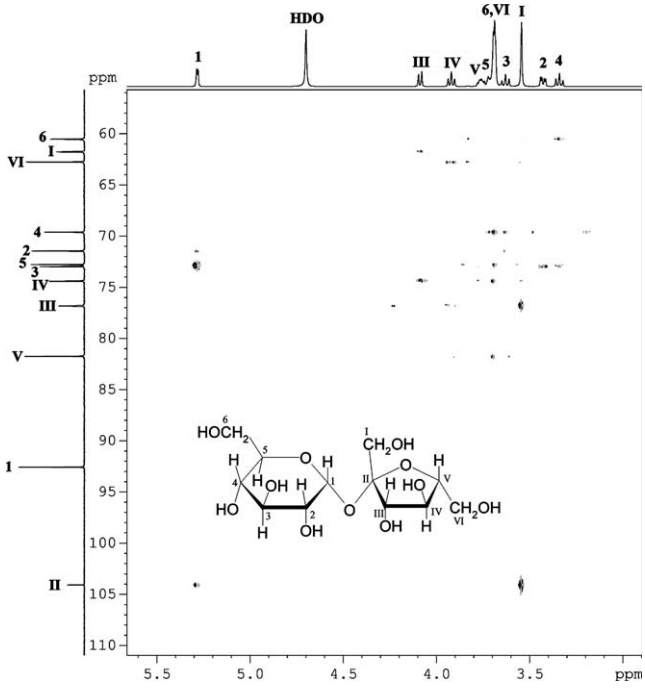

Fig. 3. 500 MHz LR-CAHSQC spectrum of sucrose. The experimental details are described in the text and in the caption of Fig. 1.

$-J_{CH}/2$ [2]. The J_{CH} coupling values were acquired from the literature [31]. In a true situation for a molecule with unknown couplings, the ${}^{n}J_{CH}$ is determined by iterative manner; e.g., by changing the trial J_{CH} and monitoring when the deviation between trial reference spectrum and F2-projection is minimum.

A general inspection shows no difference in the sensitivity and qualitative information between the LR-HSQC and LR-CAHSQC spectra. However, a closer examination reveals some anomalies in LR-HSQC spectra. Expansions of two long-range correlation peaks, C^{I},H^{III} ($^{3}J_{CH}$) and C^{6},H^{4} ($^{3}J_{CH}$), and their behavior as the function of J_{opt} are shown in Fig. 4. The

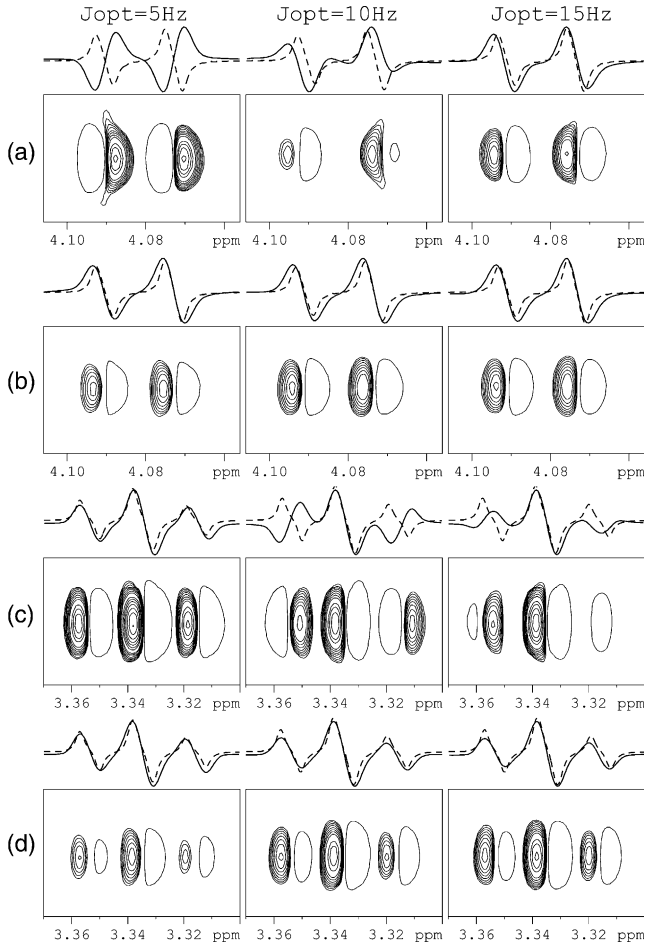

Fig. 4. Expansions of 2D long-range correlation spectra of sucrose obtained with LR-HSQC (a and c) and LR-CAHSQC (b and d) pulse sequences. The spectra are plotted at the same intensity levels. For the negative signals, only one contour level is shown. The F2-projection is shown on top of the spectrum (solid line), and the simulated reference spectrum is plotted with a dashed line. The expansions are from the C^{I},H^{III} ($^{3}J_{CH} = 3.2$ Hz) correlation peak of LR-HSQC (a) and LR-CAHSQC (b) spectra, and from the C^{6},H^{4} ($^{3}J_{CH} = 3.5$ Hz) correlation peak of LR-HSQC (c) and LR-CAHSQC (d) spectra optimized for the heteronuclear long-range couplings of 5, 10, and 15 Hz (J_{opt}). Homonuclear vicinal couplings found from the proton resonances are 7.8 Hz (H^{III},H^{IV}) and 9.4 Hz (H^{4},$H^{3,5}$).

phase properties of the doublet signal (H^{III}) in LR-HSQC spectra (Fig. 4a) are good in spectrum optimized for $J_{opt} = 15$ Hz and the long-range ^{1}H–^{13}C coupling can be easily obtained using a reference spectrum constructed from a normal ^{1}H spectrum. In the spectrum recorded with $J_{opt} = 5$ Hz, the phase is shifted by 180° as was anticipated by the Fig. 2. This can be an unexpected surprise when forming the reference spectrum, but the coupling constant can still be extracted accurately. However, when the J_{opt} is close to the homonuclear coupling constant (10 Hz), the shape of the correlation peak does not match with the reference spectrum and accurate evaluation of coupling constant is difficult. Accordingly, the phase properties of the triplet peak of H^{4} in LR-HSQC spectrum (Fig. 4c) are good when spectrum is acquired with J_{opt} of 5 Hz, and the coupling constant can be easily evaluated. Again, when J_{opt} (10 Hz) approaches the value of homonuclear coupling constant (9.4 Hz), the phase of the resulting correlation peak does not agree with the reference spectrum, i.e., the correlation peak multiplet is antiphase with respect to both J_{HH} and J_{CH} coupling, as expected according to the Eq. (4) (the term $H_y H'_z H''_z C_z$ dominates). Furthermore, the phase anomaly is still present in the spectrum optimized for long-range coupling of 15 Hz. The phase characteristics of the LR-CAHSQC spectra (Figs. 4b and d) are good regardless of the J_{opt}, and therefore the coupling constant evaluation is straightforward.

In conclusion, the LR-CAHSQC is more tolerant to the phase anomalies caused by homonuclear coupling than normal LR-HSQC, and thus less attention to the size of homonuclear coupling need to be paid when planning suitable J_{opt} for the experiment. The evaluation of long-range coupling constants can be performed by employing a normal ^{1}H spectrum as the reference spectrum or, in feasible cases when line width is smaller, directly from the antiphase peak separation.

4. Experimental

The experiments were performed at 300 K with a Bruker DRX-500 NMR spectrometer equipped with a 5-mm broadband inverse probehead with z-gradient. The sucrose sample was prepared by dissolving 68 mg of sucrose in 0.5 ml of 99.5%-deuterated D_2O.

The LR-CAHSQC and LR-HSQC spectra from sucrose were acquired by measuring 16 scans per increment, with total of 500 increments. The number of dummy scans was 64. A squared cosine window function was applied on both dimensions prior to Fourier transform. The size of transformed spectrum was $8k * 1k$. All spectra were phased by reference to the H^{I},C^{III} correlation peak, so as to give an antiphase peak shape resulting from the $^{3}J_{CH}$ coupling.

References

[1] A. Bax, M.F. Summers, ^{1}H and ^{13}C assignments from sensitivity-enhanced detection of heteronuclear multiple-bond connectivity by 2D multiple quantum NMR, J. Am. Chem. Soc. 108 (1986) 2093–2094.

[2] J. Keeler, D. Neuhaus, J.J. Titman, A convenient technique for the measurement and assignment of long-range carbon-13 proton coupling constants, Chem. Phys. Lett. 146 (1988) 545–548.

[3] J.J. Titman, D. Neuhaus, J. Keeler, Measurement of long-range heteronuclear coupling constants, J. Magn. Reson. 85 (1989) 111–131.

[4] J.M. Richardson, J.J. Titman, J. Keeler, D. Neuhaus, Assesment of a method for the measurement of long-range heteronuclear coupling constants, J. Magn. Reson. 93 (1991) 533–553.

[5] S. Sheng, H. van Halbeek, Accurate and precise measurement of heteronuclear long-range couplings by a gradient-enhanced two-dimensional multiple-bond correlation experiment, J. Magn. Reson. 130 (1998) 296–299.

[6] G. Bodenhausen, D.J. Ruben, Natural abundance ^{15}N NMR by enhanced heteronuclear spectroscopy, Chem. Phys. Lett. 69 (1980) 185–189.

[7] R. Marek, L. Krailik, V. Sklenar, Gradient-enhanced HSQC experiments for phase-sensitive detection of multiple bond interactions, Tetrahedron Lett. 38 (1997) 665–668.

[8] R.T. Williamson, B.L. Marquez, W.H. Gerwick, K.E. Köver, One- and two-dimensional gradient-selected HSQMBC NMR experiments for the efficient analysis of long-range heteronuclear coupling constants, Magn. Reson. Chem. 38 (2000) 265–273.

[9] W.R. Croasmun, R.M.K. Carlson, Two-Dimensional NMR Spectroscopy: Applications for Chemists and Biochemists, second ed., VCH Publishers, New York, 1994, pp. 482–483.

[10] H.Y. Carr, E.M. Purcell, Effects of diffusion on free precession in nuclear magnetic resonance experiments, Phys. Rev. 94 (1954) 630–638.

[11] S. Meiboom, D. Gill, Modified spin–echo method for measuring nuclear relaxation times, Rev. Sci. Instrum. 29 (1958) 688–691.

[12] R.L. Vold, J.S. Waugh, M.P. Klein, D.E. Phelps, Measurement of spin relaxation in complex system, J. Chem. Phys. 48 (1968) 3831–3832.

[13] J.W. Peng, V. Thanabal, G. Wagner, Improved accuracy of heteronuclear transverse relaxation time measurements in macromolecules. Elimination of anti-phase contributions, J. Magn. Reson. 95 (1991) 421–427.

[14] R. Ishima, J.M. Louis, D.A. Torchia, Transverse ^{1}H cross relaxation in ^{1}H–^{15}N correlated ^{1}H CPMG experiments, J. Magn. Reson. 137 (1999) 289–292.

[15] S. Heikkinen, I. Kilpeläinen, Linewidth-resolved ^{15}N HSQC, a simple 3D method to measure ^{15}N relaxation times from T_1 and T_2 linewidths, J. Magn. Reson. 151 (2001) 314–319.

[16] A. Allerhand, Analysis of Carr–Purcell spin–echo NMR experiments on multiple-spin systems. I: the effect of homonuclear coupling, J. Chem. Phys. 44 (1966) 1–9.

[17] R.R. Ernst, G. Bodenhausen, A. Wokaun, Principles of Nuclear Magnetic Resonance in One and Two Dimensions, Clarendon Press, Oxford, 1990, pp. 206–209.

[18] T. Gullion, D.B. Baker, M.S. Conradi, New, compensated Carr–Purcell sequences, J. Magn. Reson. 89 (1990) 479–484.

[19] S.J. Glaser, J.J. Quant, Homonuclear and heteronuclear Hartmann–Hahn transfer in isotropic liquids, Adv. Magn. Opt. Reson. 19 (1996) 59–252.

[20] R.D. Bertrand, W.B. Moniz, A.N. Garroway, G.C. Chingas, ^{13}C–^{1}H cross-polarization in liquids, J. Am. Chem. Soc. 100 (1978) 5227–5229.

[21] L. Müller, R.R. Ernst, Coherence transfer in the rotating frame. Application to heteronuclear cross-correlation spectroscopy, Mol. Phys. 38 (1979) 963–992.

[22] P. Pelupessy, E. Chiarparin, Hartmann–Hahn polarization transfer in liquids: an ideal tool for selective experiments, Concepts Magn. Reson. 12 (2000) 103–124.

[23] B. Luy, J.P. Marino, ^{1}H–^{31}P CPMG-correlated experiments for the assignment of nucleic acids, J. Am. Chem. Soc. 123 (2001) 11306–11307.

[24] L. Mueller, P. Legault, A. Pardi, Improved RNA structure determination by detection of NOE contacts to exchange-broadened amino protons, J. Am. Chem. Soc. 117 (1995) 11043–11048.

[25] F.A.A. Mulder, C.A.E.M. Spronk, M. Slijper, R. Kaptein, R. Boelens, Improved HSQC experiments for the observation of exchange broadened signals, J. Biomol. NMR 8 (1996) 223–228.

[26] K. Ogura, H. Terasawa, F. Inagaki, An improved double-tuned and isotope-filtered pulse scheme based on a pulsed field gradient and a wide-band inversion shaped pulse, J. Biomol. NMR 8 (1996) 492–498.

[27] E.J. Wells, H.S. Gutowsky, NMR spin–echo trains for a coupled two-spin system, J. Chem. Phys. 43 (1965) 3414–3415.

[28] L. Braunschweiler, R.R. Ernst, Coherence transfer by isotropic mixing: application to proton correlation spectroscopy, J. Magn. Reson. 53 (1983) 521–528.

[29] D.G. Davis, A. Bax, Assignment of complex ^{1}H NMR spectra via two-dimensional homonuclear Hartmann–Hahn spectroscopy, J. Am. Chem. Soc. 107 (1985) 2820–2821.

[30] R.P. Hicks, J.K. Young, D. Moskau, Magnetization transfer via isotropic mixing: an introduction to the HOHAHA experiment, Concepts Magn. Reson. 6 (1994) 115–130.

[31] F.G. Vogt, A.J. Benesi, 1D determination of long-range heteronuclear coupling constants by gradient enhanced SIMBA, J. Magn. Reson. 132 (1998) 214–219.